Chemical Engineering Journal 165 (2010) 379–387

Contents lists available at ScienceDirect

Chemical Engineering Journal

journal homepage: www.elsevier.com/locate/cej

Review

Effect of phase dispersion and mass transfer direction on steady state RDC performance using population balance modelling

Moutasem Jaradat[a,c], Menwer Attarakih[a,b], Hans-Jörg Bart[a,c,*]

[a] Lehrstuhl für Thermische Verfahrenstechnik, TU Kaiserslautern, P.O. Box 3049, 67653 Kaiserslautern, Germany
[b] Faculty of Engineering Technology, Chemical Engineering Department, Al-Balqa Applied University, P.O. Box 15008, 11134 Amman, Jordan
[c] Center of Mathematical and Computational Modelling, TU Kaiserslautern, Germany

ARTICLE INFO

Article history:
Received 5 May 2010
Received in revised form 18 August 2010
Accepted 26 September 2010

Keywords:
Hydrodynamics
Phase dispersion
Mass transfer direction
Simulation
Population balances

ABSTRACT

In this work, the steady state performance of an RDC column is studied taking into account the effect of dispersed phase inlet (light or heavy phase is dispersed) and the direction of mass transfer (from continuous to dispersed phase and vice versa) using the population balance framework. *LLECMOD*, a program that uses multivariate population balance models, is extended to take into account the direction of mass transfer and the dispersed phase inlet. It is used to simulate pilot plant RDC columns where the steady state mean flow properties (dispersed phase hold up and droplet mean diameter) and the solute concentration profiles are compared to the available experimental data. Three chemical systems were used: sulpholane–benzene–n-heptane, water–acetone–toluene and water–acetone–n-butyl acetate. The dispersed phase inlet and the direction of mass transfer as well as the chemical system physical properties are found to have profound effect on the steady state performance of the RDC column. For example, reduced mean droplet diameter is found to persist when the heavy phase is dispersed and the extractor efficiency is higher when the direction of mass transfer is from the continuous to the dispersed phase. For the purpose of experimental validation, it is found that *LLECMOD* predictions are in good agreement with the available experimental data concerning: dispersed phase hold up, mean droplet diameter and solute concentration profiles in both phases.

1. Introduction

In liquid–liquid contacting equipment, consisting of completely mixed or differential stages [1–5], droplet population balance based-modelling is now being used to describe complex interactions of coupled hydrodynamics and mass transfer. This is due to the nature of the macroscopic dispersed phase interactions (breakage and coalescence) coupled with microscopic ones (diffusional solute transfer) in a continuous turbulent flow field, which result in a population of droplets. This population is distributed not only in the spatial domain of the contacting equipment but also randomly distributed with respect to the droplet state (properties) such as size, concentration and age [1–3]. In such equipment, the dynamically changing behaviour of the dispersed phase droplets makes it necessary to consider a detailed mathematical rather than lumped modelling approach. In this connection, the population balance equation can be used to improve the column simulation by taking these details into account. The population of droplets constituting the dispersed phase is modelled in terms of a multivariate population balance equation in which the evolution processes such as breakage, coalescence and growth are taken into account. Actually, accurate prediction of the evolved dispersed phase properties depends strongly in proper modelling of these coupled processes. Consequently, the coupled hydrodynamics and mass transfer in agitated liquid–liquid extraction columns are mainly determined by the interactions between the dispersed phase constituents and the continuous phase. For realistic performance predictions, not only the dispersed phase mean properties such as holdup and droplet mean diameter are to be taken into consideration but also the evolution of the droplet size distribution along the column height. The biviariate population balance equation (with respect to droplet size and solute concentration) is proved to be an effective tool for describing steady state and dynamic extraction column performance [1,2,6,7]. Based on this framework, the population balance equation describing the coupled hydrodynamics and mass transfer in agitated liquid–liquid extraction columns was recently developed [1,8].

2. Influence of mass transfer direction

The performance of liquid–liquid extraction columns is well known to be dependent on the mass transfer direction and on the

* Corresponding author at: Lehrstuhl für Thermische Verfahrenstechnik, TU Kaiserslautern, P.O. Box 3049, 67653 Kaiserslautern, Germany.
E-mail address: bart@mv.uni-kl.de (H.-J. Bart).

1385-8947/$ – see front matter © 2010 Elsevier B.V. All rights reserved.
doi:10.1016/j.cej.2010.09.049

Nomenclature

A_c	column cross sectional area, m^2
c_x, $\bar{c}_y$	solute concentration (continuous and dispersed phase), $kg\,m^{-3}$
$\bar{D}_x$, $\bar{D}_y$	axial dispersion coefficient (continuous and dispersed phase), $m^2\,s^{-1}$
D_k, D_r, D_s	column, rotor and stator diameters, m
d, d'	droplet diameter, mm
d_{min}, d_{max}	minimum and maximum droplet diameters, mm
$f_{d,c_y}\partial d\partial c_y$	number of droplets having concentration c_y and diameter d in the range $[d, d+\partial d]\times[c_y, c_y+\partial c_y]$
H_k, H_c	column and single compartment heights, m
K_v	slowing factor
K_{oy}, $\bar{K}_{oy}$	overall and average overall mass transfer coefficient, $m\,s^{-1}$
k_x, k_y	individual mass transfer coefficient (continuous and dispersed phase), $m\,s^{-1}$
N	rotor speed, rpm, s^{-1}
Q_{bot}	total flow rate at bottom of the column, $m^3\,s^{-1}$
$Q_{x,in}$, $Q_{y,in}$	inlet flow rate (continuous and dispersed phase), $m^3\,s^{-1}$
Q_{top}	dispersed phase flow rate at top of the column, $m^3\,s^{-1}$
t	time, s
$\bar{u}_x$, $\bar{u}_y$	relative velocity (continuous and dispersed phase), $m\,s^{-1}$
$\bar{u}_r$	relative droplet (slip) velocity, $m\,s^{-1}$
$\bar{u}_t$	terminal droplet velocity, $m\,s^{-1}$
z	spatial coordinate, m
z_d, z_y	dispersed feed inlet, m
z_c, z_x	continuous phase inlet, m

Greek symbols

β_n	daughter droplet distribution based on droplet number, m^{-1}
Γ	droplet breakage frequency, s^{-1}
ε	energy dissipation, $m^2\,s^{-3}$
ζ	time and space vector
λ	coalescence efficiency
μ_x,μ_y	viscosity (continuous and dispersed phase), $kg\,m^{-1}\,s^{-1}$
ρ_x, ρ_y	density (continuous and dispersed phase), $kg\,m^{-3}$
σ	interfacial tension, $N\,m^{-1}$
v, v'	droplet volumes, m^3
v_{min}, v_{max}	minimum and maximum droplet volume, m^3
ϕ_x, ϕ_y	holdup (continuous and dispersed phase)
ϕ_e	dispersed phase hold up entrained with the continuous phase
$\vartheta(d')$	mean no. of daughter droplets from mother droplet of diameter d′.
$\Upsilon.\partial\zeta$	source term, $m^{-3}\,s^{-1}$.
ω	coalescence frequency, $m^3\,s^{-1}$
ω_R, $\omega_{R,crit}$	rotor and critical rotor speeds respectively, s^{-1}

choice of the dispersed phase (light or heavy phase is dispersed). This is one of the most important factors influencing the global efficiency of solvent extraction contactors [9]. This can be attributed to Marangoni effects caused by surface tension gradients along a droplet surface due to mass transfer [10]. The available interfacial area resulting from competition between droplet breakage and inter-droplet coalescence is sensitive to the mass transfer direction and intensity, even in the case of dilute solutions. This is illustrated, for instance, by the profiles of the Sauter mean droplet diameter (d_{32}) along the height of the extraction column [11,12]. It is also known that mass transfer and its direction have a significant effect on the size of droplet swarms. This is attributed to the fact that coalescence and breakage of droplets are markedly affected by the transfer of solute [7,13–20]. Thornton [21] and Tung and Luecke [22] indicated that the values of the characteristic velocity (when the mass transfer direction is from the dispersed to the continuous phase) were higher, and of course the holdup is lower, than those without mass transfer. This is because the direction of mass transfer affects the droplet size via its droplet coalescence behaviour [23]. As compared with a pure two component system, the mean droplet size increases when the mass transfer direction is from the dispersed to the continuous phase, and it is reduced in the case of reversing the mass transfer direction [24], indicating that droplet coalescence is dominant in this case. In the case of mass transfer from the continuous to the dispersed phase, coalescence is hindered since film drainage between the droplets is retarded and the mean droplet size is always smaller than that without solute transfer [20,25–30].

Kleczek et al. [23] confirmed that the presence of a solute in the two phase liquid system tends to lower the interfacial tension between the two immiscible liquids, and hence has a profound effect on droplet coalescence. When mass transfer occurs from the continuous to the dispersed phase, the concentration in the draining film between two approaching droplets is lower than that in the surrounding continuous phase. The resulting interfacial tension gradients retard film drainage (and hence coalescence) when the solute transfer is from the continuous to the dispersed phase; while film drainage is enhanced for the case of solute transfer from the dispersed to the continuous phase.

Concerning mass transfer rates, higher values of the mass transfer coefficients were observed during mass transfer from the dispersed to the continuous phase. This is due to the oscillations created by coalescence between interacting droplets, which is enhanced by the Marangoni effect. Huangs and Lu [31] reported that when the resistance to mass transfer is in the continuous phase, a decrease in inter-droplet distance causes a decrease of the mass transfer coefficient. Whereas, when the resistance to mass transfer is on the dispersed phase, no much variation of the mass transfer coefficient versus inter-droplet distances was found. Kumar and Hartland [32] showed that the mass transfer coefficients depend on the mass transfer direction (this is in turn affected by the inter-droplet coalescence), which for a given system is only dependent on the interfacial conditions and agitation intensity.

3. Mathematical model

In general, the spatially distributed population balance equation derived to describe the coupled hydrodynamics and mass transfer in liquid–liquid extraction columns in a one spatial domain can be written as [33]:

$$\frac{\partial f_{d,c_y}(\psi)}{\partial t}+\frac{\partial[u_y f_{d,c_y}(\psi)]}{\partial z}+\frac{\partial[\dot{c}_y f_{d,c_y}(\psi)]}{\partial c_y}$$
$$=\frac{\partial}{\partial z}\left[D_y\frac{f_{d,c_y}(\psi)}{\partial z}\right]+\frac{Q_y^{in}}{A_c}f_y^{in}(d,c_y;t)\delta(z-z_y)+\Upsilon\{\psi\} \quad (1)$$

In this equation the components of the vector $\psi=[dc_yzt]$ are those for the droplet internal coordinates (diameter and solute concentration), the external coordinate (column height), z, and time, t, where the velocity along the concentration coordinate (c_y) is $\dot{c}_y$. The source term $\Upsilon.\partial\zeta$ represents the net number of droplets produced by breakage and coalescence per unit volume and unit time in the coordinates range $[\zeta, \zeta+\partial\zeta]$. The left hand side is the continuity operator in both the external and internal coordinates, while

the first part on the right hand side is the droplets axial dispersion characterized by the dispersion coefficient, D_y, which might be dependent on the energy dissipation and the droplet rising velocity [3,13]. The second term on the right hand side is the rate at which the droplets entering the LLEC with volumetric flow rate, Q_y^{in} that is perpendicular to the column cross-sectional area, A_c, at a location z_y. This has an inlet number density, f_y^{in}, and is treated as a point source in space. The dispersed phase velocity, u_y, relative to the walls of the column is determined in terms of the relative (slip) velocity with respect to the continuous phase and the continuous phase velocity, u_x, with respect to the walls of the column as follows:

$$u_y = u_s - u_x \tag{2}$$

The slip velocity, u_s, appearing in the above equation can be related to the single droplet terminal velocity, u_t, to take into account droplet swarm (the effect of the dispersed phase hold up, ϕ_y) and the flow conditions in a specific equipment:

$$u_s = K_v(1-\phi_y)^m u_t(d,P) \tag{3}$$

The exponent m is called the velocity exponent and is a function of the droplet's Reynolds number [2,13]. The elements of the vector P consists of the system physical properties [$\mu\rho\sigma$], and K_v is a slowing factor to take into account the effect of the column internal geometry on the droplet terminal velocity ($0 < K_v \leq 1$) [3,13,34]. A useful guide for selecting the suitable droplet terminal velocity based on the shape of the droplet (rigid, oscillating or circulating), and hence on the system physical properties, can be found in Gourdon et al. [30].

The solute concentration in the continuous phase, C_x, is predicted using a component solute balance in the continuous phase [6]:

$$\frac{\partial(\phi_x c_x)}{\partial t} - \frac{\partial}{\partial z}\left(u_x\phi_x c_x + D_x\frac{\partial(\phi_x c_x)}{\partial z}\right) = \frac{Q_x^{in}c_x^{in}}{A_c}\delta(z-z_y) - \int_0^{\infty}\int_0^{c_{y,\max}} \dot{c}_y \nu(d) f_{d,c_y}(\psi)\partial d\partial c_y \tag{4}$$

Note that the volume fraction of the continuous phase, ϕ_x, satisfies the physical constraint: $\phi_x + \phi_y = 1$. The left hand side of Eq. (4) as well as the first term on the right hand side have the same interpretations as those given in Eq. (1). The last term appearing in Eq. (4) is the total rate of solute transferred from the continuous to the dispersed phase, where the liquid droplets are treated as point sources. Note that Eq. (1) is coupled to the solute balance in the continuous phase given by Eq. (4) through the convective and the source terms. The bivariate source term appearing in Eq. (1) due droplet breakage and coalescence is given in detail by Attarakih et al. [6].

4. LLECMOD program

The complete mathematical model described above is programmed using Visual Digital FORTRAN with optimized and efficient numerical algorithms. To facilitate the data input and output, a graphical user interface was designed. The graphical interface of the *LLECMOD* (Liquid–Liquid Extraction Column Module) program contains the main input window and sub-windows for parameters and correlations input. The main window contains all correlations and operating conditions that can be selected using drop down menus. The basic feature of this program [1] is to provide an easy tool for the simulation of coupled hydrodynamics and mass transfer in liquid–liquid extraction columns based on the population balance approach for both transient and steady states conditions through an interactive windows input dialog. Note that *LLECMOD* is not restricted to a certain type of liquid–liquid extraction column since it is built in the most general form that allows the user to input the various droplet interaction functions. These functions include droplet terminal velocity (taking into account the swarm effect) and the slowing factor due to column geometry, the breakage frequency and daughter droplet distribution, the coalescence frequency and the axial dispersion coefficients.

Using *LLECMOD*, simulations can now be carried out successfully for different types of extraction columns including agitated (RDC and Kühni) and nonagitated (sieve plate and packed) columns.

4.1. Droplet terminal velocity

LLECMOD has several correlations for terminal droplet velocity that can be chosen by the user. These velocity correlations are: Klee and Treybal [35], Vignes [36], Grace et al. [37], Henschke [38], and the rigid sphere law interpolated between the viscous and inertial regimes as given by Wesselingh and Bollen [39]. If the user does not choose any of these correlations, *LLECMOD* automatically chooses the suitable velocity correlation by default, based on the selection chart described in detail by Godfrey and Slater [4].

4.2. Axial dispersion coefficients

The axial dispersion coefficients ($\bar{D}_x$&$\bar{D}_y$) for the dispersed and continuous phases are defined in the user input module as functions. These coefficients are allowed to vary with the column height in the present version of *LLECMOD*. Typical published axial dispersion correlations for RDC column used in the *LLECMOD* program are listed in Ref. [1].

4.3. Breakage frequency and daughter droplet distribution

The breakage frequency function $\Gamma(d,\bar{c}_y,\phi_y)$ can be easily defined in the user input module. The existing database of *LLECMOD* contains five breakage frequency models. The droplet breakage frequency is defined as [18]:

$$\Gamma(d,\phi_y) = P_r(d,N)\frac{\left|\bar{u}_y(d,\phi_y)\right|}{H_c} \tag{5}$$

Where the breakage probability, p_r, is correlated with the system physical properties and the energy dissipation in the following form [3,7,18]:

$$\frac{p_r}{1-p_r} = 1.2\times10^{-6}\left[\frac{\rho_x^{0.8}\mu_x^{0.2}dD_R^{1.6}(2\pi)^{1.8}(N^{1.8}-N_{crit.}^{1.8})}{\sigma}\right]^{2.88} \tag{6}$$

In the above equation, $N_{R,crit}$ is the critical rotor speed below which the breakage probability falls to zero and H_c is the compartment height. The critical rotor speed is given by Schmidt et al. [7]:

$$N_{crit} = 0.016\frac{D_R^{-2/3}\eta_y d^{-4/3}}{(\rho_x\rho_y)^{1/2}} + \left[\left(0.008\frac{D_R^{-2/3}\eta_y d^{-4/3}}{(\rho_x\rho_y)^{1/2}}\right)^2 + 0.127\frac{\sigma}{\rho_x D_R^{4/3} d^{5/3}}\right]^{0.5} \tag{7}$$

The daughter droplet distribution is assumed to follow the beta distribution as given by Cauwenberg et al. [18]:

$$\beta_n(d|d') = 3\vartheta(\vartheta-1)\left[1-\left(\frac{d}{d'}\right)^3\right]^{(\vartheta-2)}\frac{d^2}{d'^3} \tag{8}$$

Table 1
Physical and chemical properties of the chemical systems used in simulation.

Physical property	Unit	Test system					
		n-Heptane + benzene mixture	Sulpholane	Toluene	Water	Butyl acetate	Water
Density	$kg\,m^{-3}$	800	1266	863.3	992.0	877.5	990.9
Viscosity	$10^{-3}\,kg\,m^{-1}\,s^{-1}$	0.8	6.0	0. 566	1.134	0.709	1.163
Interfacial tension	$N\,m^{-1}$	0.033		0.02441		0.01096	

4.4. Coalescence frequency

The physicochemical properties of the continuous phase, the direction of solute transfer and the turbulent fluctuations play an important role in droplet coalescence. It is believed that droplet coalescence occurs if the contact time between any two randomly coalescing droplets exceeds the time required for the complete intervening film drainage and rupture. In *LLECMOD* the following droplet coalescence model of Coulaloglou and Tavlarides [40] is used:

$$\omega(d, d', \phi_y, P) = c_3 \frac{\varepsilon^{1/3}}{1+\phi}(d+d')^2(d^{2/3}+d'^{2/3})^{1/2} \exp\left(-\frac{c_4 \mu_x \rho_x \varepsilon}{\sigma^2(1+\phi)^3}\left(\frac{d.d'}{d+d'}\right)^4\right) \quad (9)$$

4.5. Mass transfer coefficients

Mass transfer models depend generally on droplet internal state, where droplet circulation and oscillation can occur affecting the mass transfer performance. Thus, in *LLECMOD* the mass transfer coefficients are drop-size dependent to take into account inner circulation, presence of surfactants and the rising velocity. The mass transfer fluxes are calculated based on the two-film theory, where the individual mass transfer coefficients are defined separately for the continuous (K_x) and the dispersed (K_y) phases.

The individual mass transfer coefficients for the dispersed and continuous phases are found dependent on the behaviour of the single droplet in the sense whether it is stagnant, circulating or oscillating [41]. In *LLECMOD* many available phenomenological and experimentally correlated mass transfer models are available [42–48]. Accordingly, the suitable combination of these individual mass transfer coefficients results in the overall mass transfer coefficient, K_{oy}, which is used to predict the rate of change of solute concentration in the liquid droplet. In the present version of *LLECMOD*, the direction of mass transfer (from continuous to dispersed phase or vice versa) can be easily chosen. Moreover, the type of phase to be dispersed is also allowed to be specified by the user. This provides great flexibility in investigating the performance of liquid extraction columns.

5. Results and discussion

To investigate the effect of the dispersed phase inlet and the direction of mass transfer on the performance of an RDC extraction column, *LLECMOD* was used to perform this task. In this version of *LLECMOD* the options for changing the inlet of dispersed phase and the direction of mass transfer were added. Three chemical systems are used in the present work: The first one is a mixture of n-heptane plus benzene (light phase) and sulpholane (heavy phase) whose physical properties are shown in Table 1. The second and third ones are the standard test systems, water–acetone–toluene and water–acetone–butyl acetate [49,50]. The column operating conditions are shown in Table 2 and the external and internal column geometries are shown in Fig. 1. *LLECMOD* was extensively used to simulate the coupled hydrodynamics and mass transfer using different types of agitated columns [1,7,34]. Based on single droplet and small laboratory experiments, droplet breakage and coalescence functions were obtained from the experimental data using

Table 2
Typical operating conditions of an RDC extraction column.

RDC	Continuous top	Dispersed top
Continuous phase volumetric flow rate	$100\,l\,h$	$25\,l\,h^{-1}$
Dispersed phase volumetric flow rate	$25\,l\,h^{-1}$	$100\,l\,h^{-1}$
Mass transfer direction	c → d	d → c
Solute concentration in the continuous phase	$100\,kg\,m^{-3}$	$0\,kg\,m^{-3}$
Solute concentration in the dispersed phase	$0\,kg\,m^{-3}$	$100\,kg\,m^{-3}$

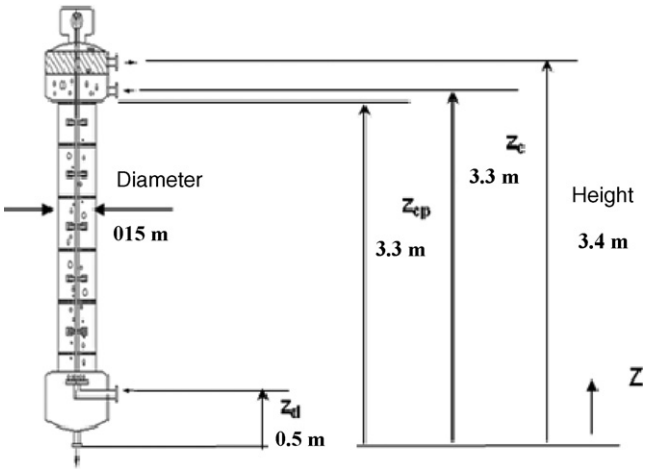

Fig. 1. External and internal geometry of the RDC column used in simulation.

different column geometries. The predictions of the program were found satisfactory in most of the simulated cases. In this section, *LLECMOD* is further validated against available experimental data [13,45] with respect to the effect of mass transfer direction and dispersion type. The RDC column diameter used for this validation is 0.1 m with a total height of 1.3 m. The dispersed and continuous phase's inlets are 0.2 and 1.2 m respectively. The column operating conditions for both mass transfer directions are shown in Table 3. It is worthwhile to mention here that the equilibrium surface tension of the chemical system (water–acetone–toluene) is available in *LLECMOD* as an empirical correlation [2]. With this the effect of

Table 3
Column operating conditions used to compare the experimental and simulated results taking into account different mass transfer directions [13,45].

RDC 100 mm	d → c, exp.	c → d, exp.
Continuous phase volumetric flow rate	$50\,l\,h^{-1}$	$60\,l\,h^{-1}$
Dispersed phase volumetric flow rate	$25\,l\,h^{-1}$	$60\,l\,h^{-1}$
Dispersion coefficient in the continuous phase	$0.000155\,m\,s^{-2}$	$0.000155\,m\,s^{-2}$
Dispersion coefficient in the dispersed phase	$0.0006520\,m\,s^{-2}$	$0.0006520\,m\,s^{-2}$
Solute concentration in the continuous phase	0.0%	6.0%
Solute concentration in the dispersed phase	5.5%	0.0%
Rotor speed	$17\,s^{-1}$	$11\,s^{-1}$

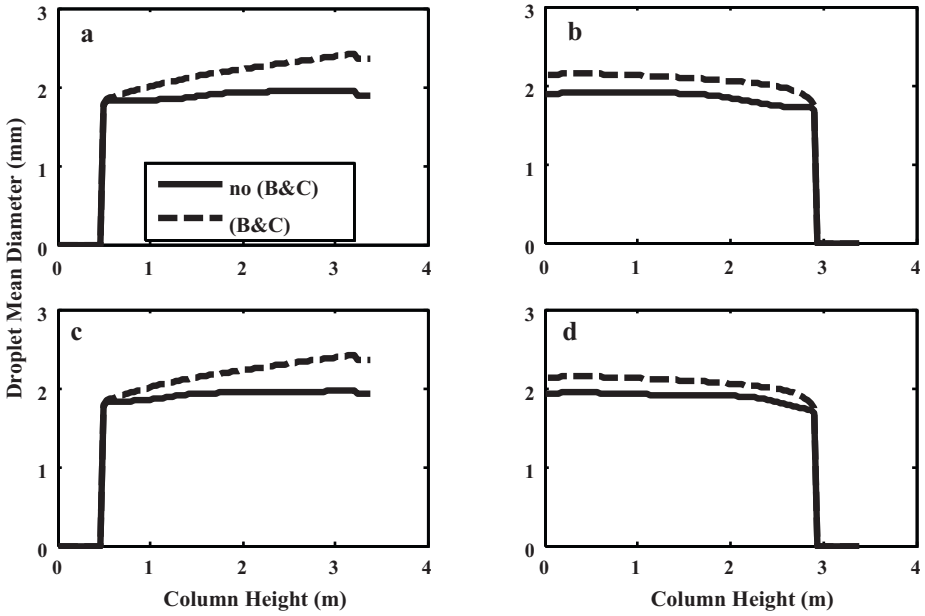

Fig. 2. Droplet mean diameter along column height without and with droplet breakage and coalescence (B&C). Mass transfer direction: (a) From heavy to light (dispersed). (b) From heavy (dispersed) to light. (c) From light (dispersed) to heavy. (d) From light to heavy (dispersed) phase.

interfacial tension on droplet breakage probability can be taken into account, which is profoundly affected by the mass transfer direction [7].

All the simulations using *LLECMOD* were run until steady state conditions (with respect to mass transfer) were reached. First, the effect of the dispersed phase inlet (which phase to be dispersed: light or heavy phase) on the column hydrodynamics (flow variables) is investigated. Fig. 2 shows the effect of the dispersed phase inlet on the mean droplet size and the average dispersed phase holdup along the column height (the phases inlets are clear from the jump discontinuities in these profiles). First, the effect of dispersed phase inlet is studied by neglecting droplet breakage and coalescence. It is well known that the droplet terminal velocity is inversely proportional to the continuous phase density and viscosity [4]. It seems that the droplet terminal velocity is more affected by the continuous phase viscosity when compared to the dispersion of the light phase, which results in a lower terminal droplet velocity. However, the holdup is slightly higher than that when the light phase is dispersed (see Fig. 3). This is because the flow rate of the dispersed phase (heavy phase) is four times larger than that of the continuous phase (see Table 2).

Since droplet breakage and coalescence are neglected, the mean droplet diameter is approximately independent of the dispersed phase inlet because the inlet feed distribution is the same in both cases. When droplet breakage and coalescence are taken into account the predicted mean droplet diameters are slightly higher in the case of dispersing the light phase (dispersed phase inlet is at the bottom) as can be seen from Figs. 2 and 3. This can be explained

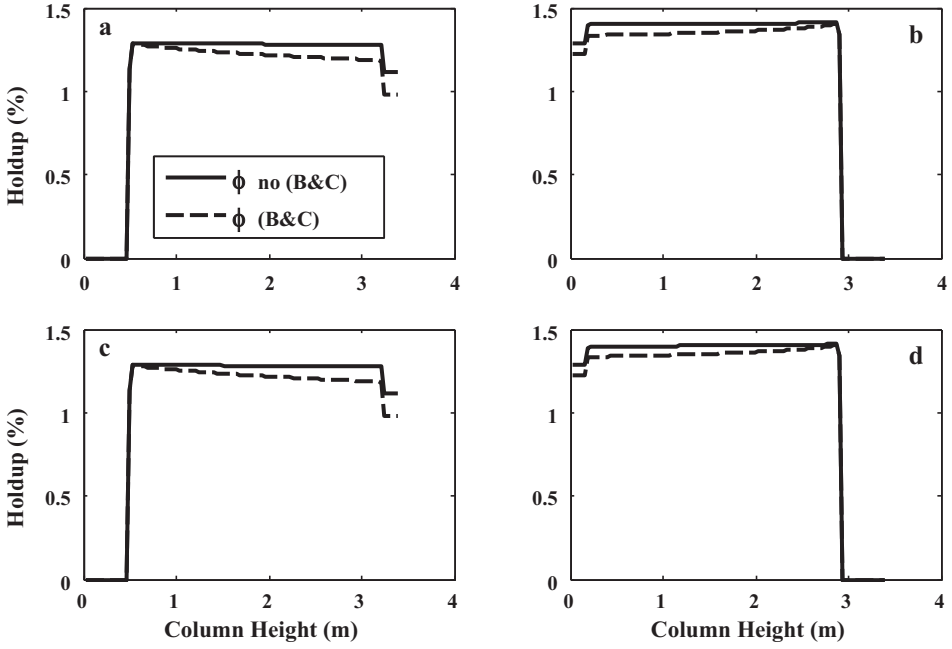

Fig. 3. Dispersed phase hold up with and without droplet breakage and coalescence (B&C): (a)–(d) are the same as those in Fig. 2.

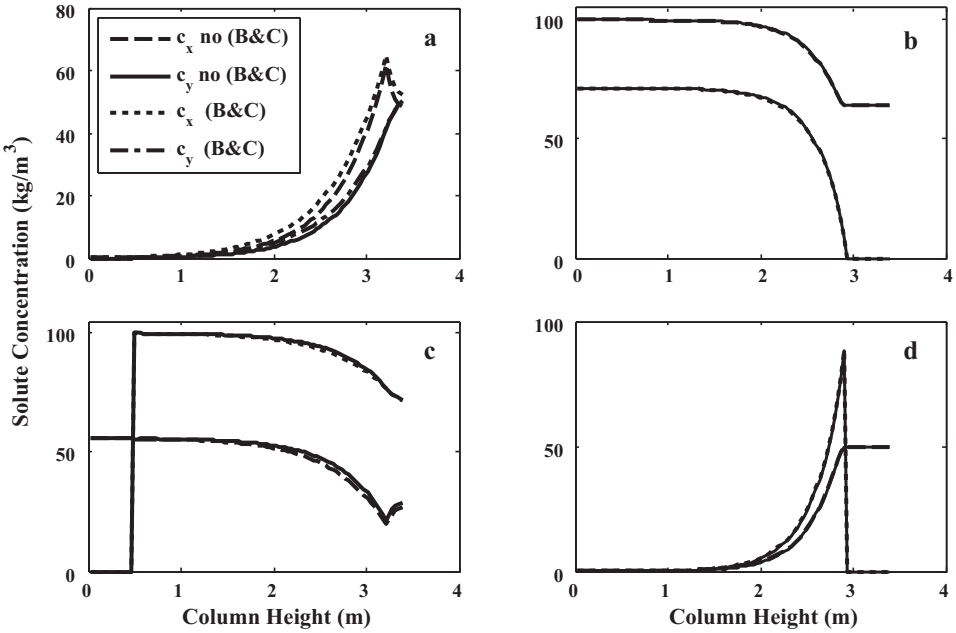

Fig. 4. Solute concentrations in the light and heavy phases with and without droplet breakage and coalescence (B&C): (a)–(d) are the same as those in Fig. 2.

by referring to the breakage probability function given by Eqs. (5) and (6). It is clear that the breakage probability is proportional to the continuous phase density. This results in more droplet breakage by the heavy continuous phase, which results in a slightly higher dispersed phase holdup as can be seen from Fig. 3. By referring to Figs. 2 and 3, the effect of mass transfer direction on the column hydrodynamics is negligible. This is because the interfacial tension (which is a critical physical property effecting droplet breakage as indicated by Eq. (6)) was assumed constant due to the lack of experimental data. On the other hand, the effect of the dispersed phase (type) inlet on the solute concentration profiles is found quite significant as can be seen from Fig. 4.

By considering the direction of mass transfer from the continuous phase to the dispersed phase, the effect of the dispersed phase inlet (at top or bottom of the column) on the solute concentration profiles is investigated as can be seen in Fig. 4a and d. It is evident that when the heavy phase is dispersed, the steady state solute removal from the heavy phase is improved when the mass transfer direction is from the continuous phase to the dispersed phase. This is clear by the reduction of the column height required for solute removal (Fig. 4d) due to the decrease in the mean droplet diameter as can be seen in Fig. 2d when compared to Fig. 2a. Since the mass transfer flux is inversely proportional to the mean droplet diameter, this increase in the extractor performance is expected. However, when the direction of mass transfer is from the dispersed phase to the continuous phase, the performance of the extraction column is improved by dispersing the heavy phase (see Fig. 4b and c). This is in fact agrees with the reduced mean droplet diameter as can be

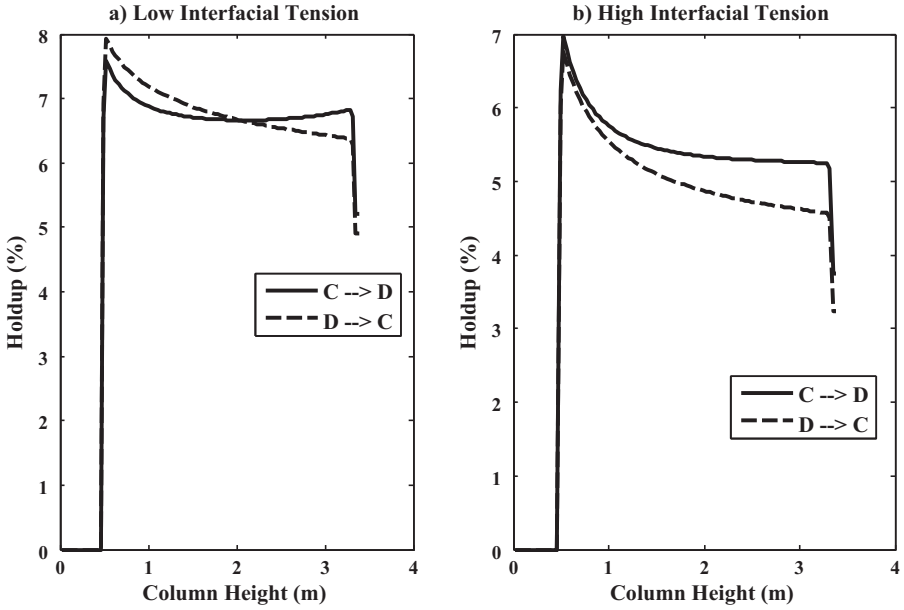

Fig. 5. Influence of mass transfer direction on holdup. The continuous and dispersed phase flow rates are 200 and 100 l h^{-1} respectively and the rotor speed is 100 rpm. (a) The chemical test system is butyl acetate–water–acetone (low interfacial tension). (b) The chemical test system is water–acetone–toluene (high interfacial tension).

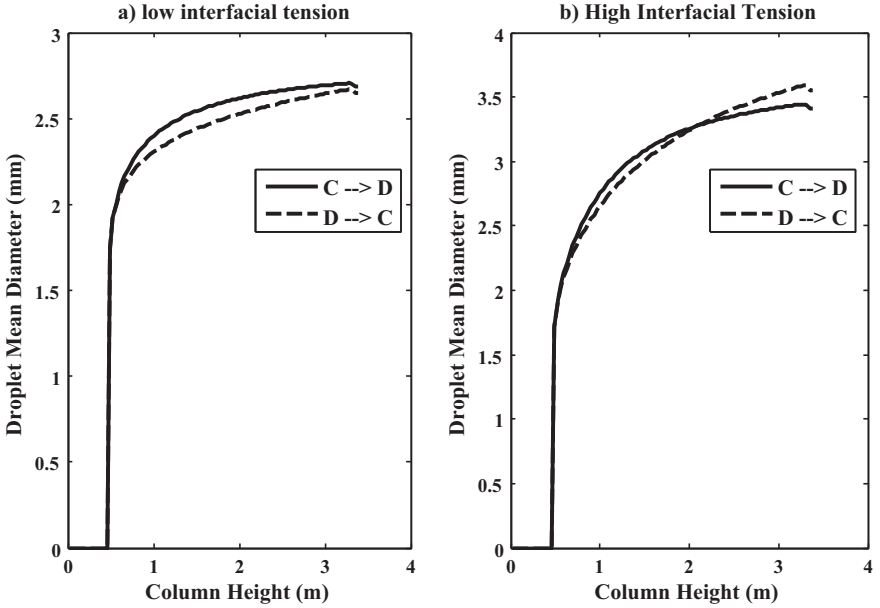

Fig. 6. Influence of mass transfer direction on droplet diameter. The continuous and dispersed phase flow rates are 200 and 100 l h^{-1} respectively and the rotor speed is 100 rpm. (a) The chemical test system is butyl acetate–water–acetone (low interfacial tension). (b) The chemical test system is water–acetone–toluene (high interfacial tension).

seen by comparing Fig. 2b and c. It is worthwhile to stress again that the Marangoni effects were not modelled in this example since the interfacial tension was kept constant. So, further discussion on the effect of mass transfer direction as reported by many researchers [51,20,52] could not be considered in this case.

To clarify the effect of the interfacial tension on the column performance (due to the dependency of droplet breakage and coalescence on interfacial tension), two chemical systems: water–acetone–toluene (high interfacial tension) and butyl acetate–water–acetone (low interfacial tension) are chosen for which the equilibrium interfacial tension are available as a function of solute concentration [2,49,50]. The other physical properties of this system are shown in Table 1. The *LLECMOD* program predicts the effect of mass transfer direction on the column hydrodynamics by providing an interfacial tension correlation as function of solute concentration along the column height [7] as shown in Figs. 5 and 6(a and b).

Fig. 5 shows the effect of the mass transfer direction on the simulated holdup profiles along the column height when the light phase is dispersed. In this figure two aforementioned chemical systems with low (butyl acetate–water–acetone) and high (water–acetone–toluene) interfacial tension are simulated. The results show that mean dispersed phase holdup is higher when the direction of mass transfer is from the continuous phase to the dispersed phase. This is due to the droplet breakage probability given by Eq. (6), which increases by a decreasing the system interfacial tension resulting in higher breakage probability. This fact is reflected by the decrease of the mean droplet diameter (especially along the upper part of the column where the rate of mass transfer is high) as can be seen in Fig. 6. Actually, this result agrees qualitatively with the experimental findings of Komasawa and Ingham [24] and Weiss et al. [19]. It should be noticed in this example that droplet coalescence is dominant at this low rotational speed (100 rpm).

The simulation results shown in Figs. 5 and 6(a and b) are carried out when the interfacial tension of both chemical systems (water–acetone–toluene and butyl acetate–water–acetone) is function of solute concentration. The models for droplet breakage probability and coalescence frequency are given by Eqs. (6) and (9) respectively. The continuous and dispersed phase flow rates are 200 and 100 l h^{-1} respectively and the rotor speed is 100 rpm.

5.1. Experimental validation

To validate the population balance model for an RDC column, steady state experimental data were compiled from the literature [13,45]. Fig. 7 compares the simulated dispersed phase (toluene) holdup to the experimental data when the direction of mass transfer is from the continuous to the dispersed phase, while Fig. 8 shows the effect of droplet breakage and coalescence on the simulated mean droplet diameter. It is clear that the error increases by neglecting droplet breakage and coalescence. The relative error was less than 15% which is a good achievement when compared to the many and often conflicting correlations in the literature [32,53,54].

The effect of mass transfer direction on the simulated and experimental solute concentration profiles is depicted in Figs. 9 and 10. As can be seen from Fig. 9, *LLECMOD* predictions of the solute profiles is in good agreement with experimental data when the mass trans-

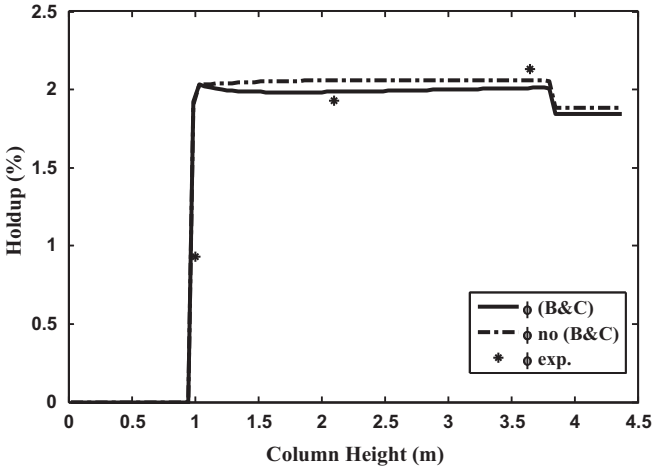

Fig. 7. Simulated and experimental [13] dispersed phase hold up as function of column height. Mass transfer direction from continuous to dispersed.

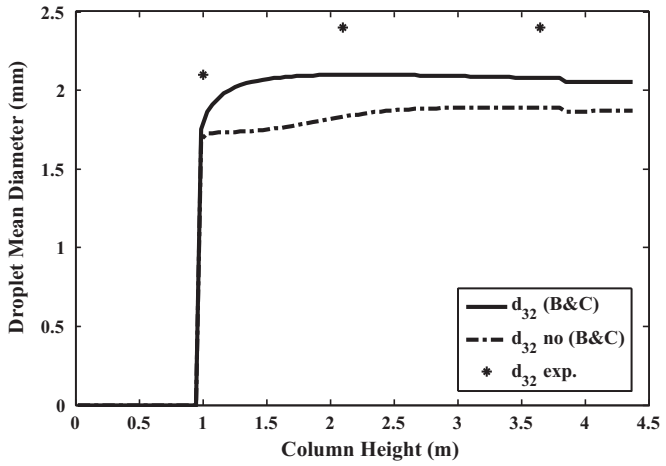

Fig. 8. Simulated and experimental [13] mean droplet diameter as function of column height. Mass transfer from continuous to dispersed.

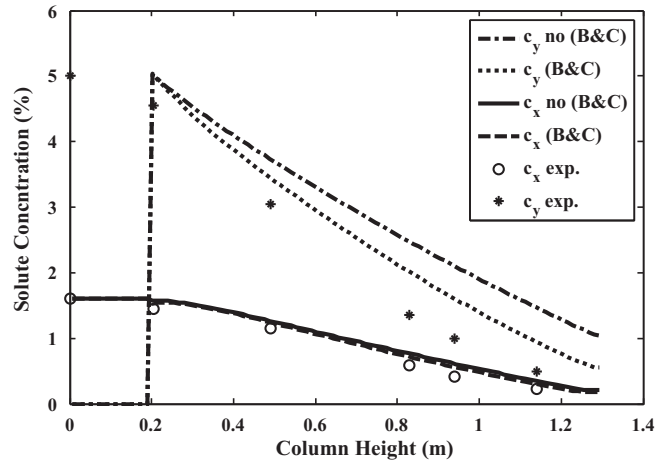

Fig. 9. Simulated and experimental [45] solute concentration profiles as function of the column height. Mass transfer from dispersed to continuous.

fer direction is from the dispersed to the continuous phase [45]. Similarly, the experimental data of Garthe [13] were compared to *LLECMOD* simulations when the mass transfer direction is from the continuous to the dispersed phases as depicted in Fig. 10. Note that

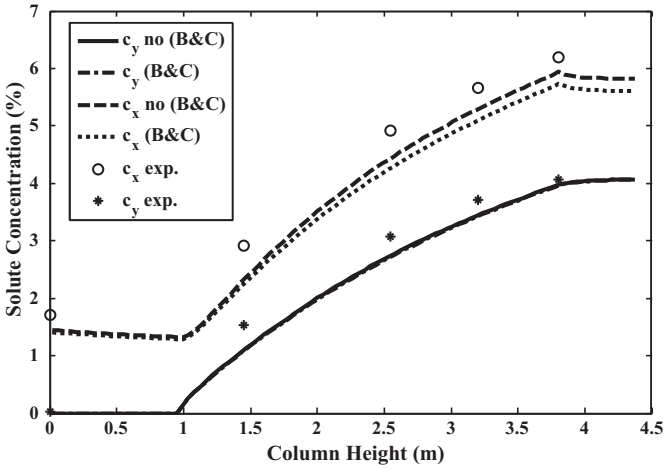

Fig. 10. Simulated and experimental [13] solute concentration profiles as function of the column height. Mass transfer from continuous to dispersed.

the mean properties of the dispersed phase are always less accurate than that of the continuous one as observed by Attarakih et al. [1] and Schmidt et al. [7]. This may be attributed to the difficulty in measurement of the dispersed phase properties. Anyhow, the error in the predicted solute concentration profiles is less than 10%. It should be mentioned at this point that the column performance is better when the mass transfer direction is from the continuous to the dispersed phase. This is in agreement to the published literature since droplet breakage is enhanced leading to an increase in the interfacial area available for mass transfer [16].

6. Summary and conclusions

It is shown in this work that the performance of Rotating Disk Contactor (RDC) depends strongly on the dispersed phase properties that dictate the interfacial area available for mass transfer. Since this interfacial area depends on the evolution of the dispersed phase population, classical or lumped models fail when competing with detailed population balance modelling. The effect of the spatial change of dispersed phase properties and their mutual influence on column hydrodynamics and mass transfer is now possible in the *LLECMOD* program. The present version of *LLECMOD* offers the options of dispersing either the light or heavy phases where reduced mean droplet diameter is found to persist when the heavy phase is dispersed. The steady state performance of an RDC extraction column is studied using a detailed population balance framework as an alternative to the commonly applied dispersion and backmixing models. So, one can draw the following conclusions:

(1) The experimental and simulation results show that there is a profound effect of mass transfer direction on the liquid–liquid extraction column performance. This is generally cannot be simulated without taking into account droplet size distribution and the coupled hydrodynamics and mass transfer through the system interfacial tension.
(2) With respect to the mass transfer direction it is found that the extractor efficiency is higher when the direction of mass transfer is from the continuous to the dispersed phase, which agrees with the published experimental data.
(3) The predicted steady state mean properties of the dispersed phase were found less accurate than that of the continuous phase mean properties when compared to the experimental data. This may be attributed to the accuracy of the measuring techniques used in the experiments.

Acknowledgments

The authors acknowledge the financial support from DFG (Deutsche Forschungsgemeinschaft), Bonn and DAAD (Deutscher Akademischer Austauschdienst), Bonn.

References

[1] M.M. Attarakih, H.-J. Bart, T. Steinmetz, M. Dietzen, N.M. Faqir, LLECMOD: a bivariate population balance simulation tool for liquid–liquid extraction columns, Open Chem. Eng. J. 2 (2008) 10–34.
[2] A. Gerstlauer, Herleitung und Reduktion populationsdynamischer Modelle am Beispiel der Flüssig-Flüssig-Extraktion, Fortschritt-Berichte VDI (1999).
[3] G. Modes, H.-J. Bart, D. Rodrigues-Peranchoand, D. Bröder, Simulation of the fluid dynamics of solvent extraction columns from single droplet parameters, Chem. Eng. Technol. 22 (3) (1999) 231–236.
[4] J.C. Godfrey, M.J. Slater (Eds.), Liquid–Liquid Extraction Equipment, Wiley & Sons, Chichester, 1994.
[5] T.C. Lo, M.H.I. Baird, C. Hanson (Eds.), Handbook of Solvent Extraction, Wiley & Sons, New York, 1983.
[6] M.M. Attarakih, H.-J. Bart, N.M. Faqir, Numerical solution of the bivariate population balanced equation for the interacting hydrodynamics and mass transfer in liquid–liquid extraction columns, Chem. Eng. Sci. 61 (2006) 113–123.

[7] A.S. Schmidt, M. Simon, M.M. Attarakih, L.G. Lagar, H.-J. Bart, Droplet population balance modelling: hydrodynamics and mass transfer, Chem. Eng. Sci. 61 (2006) 246–256.
[8] M.M. Attarakih, H.-J. Bart, N.M. Faqir, A hybrid scheme for the solution of the bivariate spatially distributed population balanced equation, Chem. Eng. Technol. 29 (2006) 435–441.
[9] A. Saboni, C. Gourdon, A.K. Chesters, The influence of inter-phase mass transfer on the drainage of partially mobile liquid films between drops undergoing a constant interaction force, Chem. Eng. Sci. 54 (1999) 461–473.
[10] J.C. Godfrey, M.J. Slater, Slip velocity relationships for liquid–liquid extraction columns, Trans. Inst. Chem. Eng. 69 (1991) 130–141.
[11] C. Gourdon, Les Colonnes d'Extraction par Solvant: Modèlesetcomportement, Dissertation, Institute National Polytechnique de Toulouse, Toulouse, 1989.
[12] C. Gourdonand, G. Casamatta, Influence of mass transfer direction on the operation of a pulsed sieve-plate pilot column, Chem. Eng. Sci. 46 (11) (1991) 2799–2808.
[13] D. Garthe, Fluiddynamics and mass transfer of single particles and swarms of particles in extraction column, Dissertation, TU München, München, 2006.
[14] A.J. Madden, G.L. Damerell, Coalescence frequencies in agitated liquid–liquid systems, AIChE J. 8 (2) (1962) 233–239.
[15] H.F. Johnson, H. Bliss, Liquid–liquid extraction in spray towers, Trans. Am. Inst. Chem. Eng. 42 (1946) 331–358.
[16] H. Groothuis, F.J. Zuiderweg, Influence of mass transfer on coalescence of drops, Chem. Eng. Sci. 12 (1960) 288–289.
[17] D.H. Logsdail, J.D. Thornton, Liquid–liquid extraction. Part XIV: the effect of column diameter upon the performance and throughput of pulsed plate columns, Trans. Inst. Chem. Eng. 35 (1957) 331–342.
[18] V. Cauwenberg, J. Degreve, M.J. Slater, The interaction of solute transfer, contaminates and drop break-up in rotating disc contactors: Part I. Correlation of drop breakage probabilities, Can. J. Chem. Eng. 75 (1997) 1046–1055.
[19] J. Weiss, L. Steiner, S. Hartland, Determination of actual drop velocities in agitated extraction columns, Chem. Eng. Sci. 50 (2) (1995) 255–261.
[20] A. Prabhakar, G. Sriniketan, Y.B.G. Varma, Dispersed phase holdup and drop size distribution in pulsed plate columns, Can. J. Chem. Eng. 66 (1988) 232–240.
[21] J.D. Thornton, Liquid–liquid extraction. Part XIII: the effect of pulse wave form and plate geometry on the performance and throughput of a pulsed column, Trans. Inst. Chem. Eng. 35 (1957) 136–330.
[22] L.S. Tung, R.H. Luecke, Mass transfer and drop sizes in pulsed-plate extraction columns, Ind. Eng. Chem. Process Des. Dev. 25 (1986) 664–673.
[23] F. Kleczek, V. Cauwenberg, P.V. Rompay, Effect of mass transfer on droplet size in liquid–liquid dispersions, Chem. Eng. Technol. 12 (1989) 395–399.
[24] J. Komasawa, J. Ingham, Effect of system properties on the performance of liquid–liquid extraction columns-II, Chem. Eng. Sci. 33 (1978) 479–485.
[25] P.M. Bapat, L.L. Tavlarides, Mass transfer in a liquid–liquid CFSTR, AIChE J. 31 (4) (1985) 659–666.
[26] A.K. Bensalem, Hydrodynamics and mass transfer in a reciprocating plate extraction column, Dissertation, Swiss Federal Institute of Technology, Zurich, 1985.
[27] C. Marangoni, Difesa della teoria dell'elasticità superficiale dei liquidi. Plasticità superficiale, Il Nuovo Cimento 3 (1) (1878) 193–211.
[28] C. Marangoni, Sul principio della viscosità super ficiale dei liquidi stabilito dal sig. Plateau, Nuovo Cimento 2 5/6 (1871) 239–273.
[29] K. Cauwenberg, J. Degreve, M.J. Slater, The interaction of solute transfer, contaminants and drop break-up in rotating disc contactors: Part II. The coupling of the mass transfer and breakage processes via interfacial tension, Can. J. Chem. Eng. 75 (1997) 1056–1066.
[30] C. Gourdon, G. Casamatta, G. Muratet, Population balance based modelling of solvents extraction columns, in: J.C. Godfrey, M.J. Slater (Eds.), Liquid–Liquid Extraction Equipment, Wiley & Sons, New York, 1994, pp. 137–226.
[31] Y.-Y. Huangs, M. Lu, Continuous phase mass transfer coefficients for single droplets moving in an infinite droplet chain, Chem. Eng. Commun. 171 (1) (1999) 181–194.
[32] A. Kumar, S. Hartland, Mass transfer in a Kühni extraction column, Ind. Eng. Chem. Res. 27 (1988) 1198–1203.
[33] M.M. Attarakih, H.-J. Bart, N.M. Faqir, LLECMOD: a windows-based program for hydrodynamics simulation of liquid–liquid extraction columns, Chem. Eng. Process. 45 (2) (2006) 113–123.
[34] T. Steinmetz, S.A. Schmidt, H.-J. Bart, Modellierung gerührter Extraktionskolonnen mit dem Tropfenpopulationsbilanzmodell, Chem. Ing. Technol. 77 (6) (2005) 723–733.
[35] A.J. Klee, R.E. Treybal, Rate of rise or fall of liquid drops, AIChE J. 2 (1956) 444–447.
[36] A. Vignes, Hydrodynamique des dispersions, Genie Chim. 93 (1965) 129–142.
[37] J.R. Grace, T. Wairegi, T.H. Nguyen, Shapes and velocities of single drops and bubbles moving freely through immiscible liquids, Trans. Inst. Chem. Eng. 54 (1976) 167–173.
[38] M. Henschke, Auslegung pulsierter Siebboden-Extraktionskolonnen, RWTH Aachen, Habilitationsschrift, 2003.
[39] J.A. Wesselinghand, A.M. Bollen, Single particles, bubbles and drops: their velocities and mass transfer coefficients, Trans. Inst. Chem. Eng. 77 (1999) 89–96.
[40] C.A. Coulaloglou, L.L. Tavlarides, Description of interaction processes in agitated liquid–liquid dispersions, Chem. Eng. Sci. 32 (1977) 1289–1297.
[41] A. Kumarand, S. Hartland, Correlations for prediction of mass transfer coefficients in single drop systems and liquid–liquid extraction columns, Trans. Inst. Chem. Eng. 77 (A) (1999) 372–384.
[42] A.B. Newman, The drying of porous solids diffusion and surface emission equations, AIChE J. 27 (1931) 203–220.
[43] A.E. Handlos, T. Baron, Mass transfer from drops in liquid extraction, AIChE J. 3 (1957) 127–136.
[44] R. Kronig, J. Brink, On the theory of extraction from falling droplets, Appl. Sci. Res. A2 (1950) 142–154.
[45] B.H. Wolschner, Konzentrationsprofile in Drehscheibenextraktoren, Dissertation, Technische UniversitätGraz, Graz, 1980.
[46] W.J. Korschinsky, C.H. Young, Modelling drop-side mass transfer in agitated polydispersed liquid–liquid systems, Chem. Eng. Sci. 40 (1989) 2355–2361.
[47] M.J. Slater, A combined model of mass transfer coefficients for contaminated drop liquid–liquid systems, Can. J. Chem. Eng. 73 (1995) 462–469.
[48] H.-J. Bart, Reactive Extraction, Springer, Berlin, 2001.
[49] T. Misek (Ed.), Recommended Systems for Liquid–Liquid Extraction Studies, European Federation of Chemical Engineering, Working Party on Distillation, Absorption and Extraction, The Institution of Chemical Engineers, Rugby, 1978.
[50] T. Misek, R. Berger, J. Schröter (Eds.), Standard Test Systems for Liquid–Liquid Extraction, European Federation of Chemical Engineering, Working Party on Distillation, Absorption and Extraction, The Institution of Chemical Engineers, Rugby, 1985.
[51] Z.J. Shen, N.V. Ramarao, M.H.I. Baird, Mass transfer in a reciprocating plate extraction column—effects of mass transfer direction and plate material, Can. J. Chem. Eng. 63 (1) (1985) 29–36.
[52] D. Venkatanarasaiah, Y.B.G. Varma, Dispersed phase holdup and mass transfer in liquid pulsed column, Bioprocess. Biosyst. Eng. 18 (1988) 119–126.
[53] A. Kumar, S. Hartland, Prediction of drop size in rotating disc extractors, Can. J. Chem. Eng. 64 (1986) 915–924.
[54] A. Kumar, S. Hartland, Empirical prediction of operating variables, in: J.C. Godfrey, M.J. Slater (Eds.), Liquid–Liquid Extraction Equipment, Wiley & Sons, Chichester, 1994, pp. 141–226.